The LHC upper bounds for $pp \rightarrow$ diboson, $t\bar{t}$ cross section on fermionic dark matter

Karim Ghorbani[*]

Physics Department, Faculty of Sciences, Arak University, Arak 38156-8-8349, Iran

Parsa Hossein Ghorbani[†]

Institute for Research in Fundamental Sciences (IPM)
School of Particles and Accelerators, P.O. Box 19395-5531, Tehran, Iran

Abstract

The ATLAS report in August 2016 provided an upper limit for the $pp \rightarrow$ diboson and $t\bar{t}$ cross sections. We consider a pseudoscalar-mediated fermionic dark matter together with gluon and photon effective operators interacting with the pseudoscalar. Choosing the resonance mass being $m_\rho = 200, 750$ GeV and 2 TeV, beside the relic density and the invisible Higgs decay constraints we constrain more the space of parameters with the diboson and $t\bar{t}$ cross section upper bounds. We finally provide some benchmarks consistent with all the constraints. Having exploited a pseudoscalar mediator, the DM-nucleon cross section is velocity suppressed so that the model evades easily the bounds put by the future direct detection experiments such as XENON1T.

---

[*]karim1.ghorbani@gmail.com
[†]parsaghorbani@gmail.com

Contents

1 Introduction

Last year in the early LHC Run 2 data with center-of-mass energy 13 TeV, a seemingly excess in the diphoton events with the invariant mass of about 750 GeV and a best-fit width of about 45 GeV was announced by ATLAS with local significances of 3.9σ [1]. The CMS collaboration had also reported the excess [2] at diphoton invariant mass of about 760 GeV, where the best-fit gave a narrow width and a local significance of 2.6σ. If such an excess existed, similar to the discovery of the Higgs particle in 2012 [3], the new particle could be a spin-even field i.e., a spin-0 or a spin-2 (graviton) according to the Landau-Yang theorem. Unfortunately a next report by ATLAS [4] announced that the excess disappeared after analyzing more data. If it was not merely a statistical fluctuation then the first hint into beyond the standard model (BSM) had been found.

The ATLAS report [4] however still provides precious upper bounds for diboson and $t\bar{t}$ final states cross sections. In this paper we investigate if a new resonance with mass m_ρ shows up at the LHC, assuming that the resonance comes from a pseudoscalar particle decaying into diboson and $t\bar{t}$, how the fermionic dark matter scenario fits with the LHC upper bounds announced recently.

In the ATLAS report [4], the total decay width over the resonance mass, m_ρ, has been taken within $\Gamma^{\text{tot}}/m_\rho = 0.02 - 0.1$, while the resonance mass varies from 200 GeV to 6 TeV. In our computations we take the total decay width ratio to be $\Gamma^{\text{tot}}/m_\rho = 0.03 - 0.06$ and pick three samples of the resonance mass being $m_\rho = 200, 750$ GeV and 2 TeV only for illustration.

We study the case where the new resonance is a pseudoscalar and the dark matter candidate is a singlet Dirac fermion (see [5–8] for examples on fermionic DM). The pseudoscalar in this model beside interacting with the Dirac fermion dark matter and the standard model Higgs couples also to the gluons and the photon through the effective operators of dimension five we introduce in the model. The effective couplings then are bounded by the cross section upper limits at the LHC.

A special feature of having a pseudoscalar mediator in the current model is that the DM-nucleon elastic scattering cross section is velocity suppressed and the model evades easily the constraint from direct detection experiments like LUX and XENON100 or even XENON1T.

The paper is written with the following parts. In the next section we introduce the dark matter model which possesses a pseudoscalar mediator and a fermionic DM candidate. Then in section 3 we study the necessary decay widths we use in our analyses. Available constraints on the model parameter space are discussed in section 4. In section 5 we show that dark matter masses even outside the resonance region is consistence with the decay width of $25 - 45$ GeV and in the subsequent section the upper bounds on the pp cross sections are applied. We conclude the paper in section 7.

2   Pseudoscalar Mediator

In this section we introduce our model against which we will examine the diboson and $t\bar{t}$ cross section amplitude bounds obtained in the ATLAS/CMS experiments. The model includes a Dirac fermion dark matter candidate and a pseudoscalar together with two effective operators which are the sources for some of the processes measured at the LHC we analyze more in section 6.

The pseudoscalar plays the role of a mediator between the dark sector and the SM sector. We suppose that the pseudoscalar field couples to the SM fields through a gluon and a photon dimension 5 effective operators and a Higgs portal. In the effective operators the pseudoscalar is coupled to gluons and photons with dimensionful couplings at some scale Λ that we fix it latter. The dark sector Lagrangian for such a setting reads,

$$\mathcal{L}_{\text{Dark}} = \bar{\chi}(i\slashed{\partial} - m_{\text{DM}})\chi + \frac{1}{2}\partial_\mu\phi\partial^\mu\phi - \frac{m^2}{2}\phi^2 - \frac{\lambda_\phi}{4}\phi^4 \,, \tag{1}$$

where ϕ stands for the pseudoscalar and χ is the singlet Dirac fermion representing the dark matter candidate. The Lagrangian for the interactions is

$$\mathcal{L}_{\text{int}} = -ig_\chi\phi\bar{\chi}\gamma^5\chi - g_H\phi^2 H^\dagger H + c_g\frac{\alpha_s}{\pi v_H}\phi G_{\mu\nu}\tilde{G}^{\mu\nu} + c_\gamma\frac{\alpha_{em}}{\pi v_H}\phi F_{\mu\nu}\tilde{F}^{\mu\nu} \,, \tag{2}$$

where $G_{\mu\nu}$ and $F_{\mu\nu}$ are the colored $SU(3)_c$ and the electromagnetic $U(1)$ field strengths in the SM respectively. The tilde denotes the dual of the field strength, e.g., $\tilde{G}^{\mu\nu} = \frac{1}{2}\epsilon^{\mu\nu\rho\sigma}G_{\rho\sigma}$. Having in mind that ϕ, $\bar{\chi}\gamma^5\chi$, $\tilde{G}^{\mu\nu}$ and $\tilde{F}^{\mu\nu}$ are odd under CP transformation and H, $G^{\mu\nu}$ and $F^{\mu\nu}$ are CP even, the Lagrangians (1) and (2) are CP invariant.

Lagrangian (2) incorporate a pseudoscalar-Higgs quadratic interaction term. We will study these two cases separately in the following sections. Moreover, the Higgs potential in the SM sector reads,

$$V = \mu H^\dagger H + \lambda_H \left(H^\dagger H \right)^2.$$ (3)

It is worth mentioning that in the model described above, it is assumed that the pseudoscalar has a Yukawa coupling, y_x, to a vector-like exotic quark, q_x, in the fundamental representation of $SU(3)_c$ with the Lagrangian $\mathcal{L}_{\text{int}} \sim -y_x \phi q_x \gamma^5 q_x$. The effective couplings, c_g and c_γ are then generated by integrating out the vector-like quark q_x.

Moreover, the pseudoscalar couples to the SM quarks only via mixing with the SM Higgs. The coupling to the light quarks are negligible and therefore the pseudoscalar production at the LHC is dominated by the gluon fusion.

Note that even though we have not included the effective operators such as $\phi W_{\mu\nu}\tilde{W}^{\mu\nu}$ and $\phi B_{\mu\nu}\tilde{B}^{\mu\nu}$ in the Lagrangian (2), however, we can implicitly have the pseudoscalar-gauge boson couplings through the mixing of the pseudoscalar and the Higgs. The vacuum expectation value of the pseudoscalar can take a non-zero value, $\langle\phi\rangle = v_\phi$. For the Higgs particle the LHC has already fixed the mass to be $m_H \sim 125$ GeV and the Higgs vacuum expectation value is known, $v_H = 246$ GeV. Having chosen a non-zero *vev* for the pseudoscalar there is a mixing between the Higgs and the pseudoscalar. Expressing the Higgs and the pseudoscalar fields by fluctuations around their *vev*s as $\phi = v_\phi + \rho'$ and $H^\dagger = \frac{1}{\sqrt{2}}\left(0 \quad v_H + h'\right)$, and after diagonalizing the mass matrix, the mass eigenvalues (eigenstates) are described in terms of the $m_{h'}$ (field h') and $m_{\rho'}$ (field ρ') and the mixing angle θ. The mixing therefore opens a channel through which the pseudoscalar can decay into SM particles. Denoting the Higgs and the pseudoscalar mass eigenstates by h and ρ respectively, the mass eigenvalues are given as the following,

$$m_h^2 = \frac{m_{h'}^2 + m_{\rho'}^2}{2} + \frac{m_{h'}^2 - m_{\rho'}^2}{2}\sqrt{1 + y^2}\,,\, m_\rho^2 = \frac{m_{h'}^2 + m_{\rho'}^2}{2} - \frac{m_{h'}^2 - m_{\rho'}^2}{2}\sqrt{1 + y^2}\,,\quad (4)$$

where,

$$\tan(2\theta) = y = \frac{2m_{h'\rho'}^2}{m_{h'}^2 - m_{\rho'}^2}\,,\qquad m_{h'\rho'}^2 = 2g_H v_H v_\phi\,,\qquad m_{h'}^2 = 2\lambda_H v_H^2\,,\qquad m_{\rho'}^2 = 2\lambda_\phi v_\phi^2.$$ (5)

The mass eigenvalues now are taken to be the physical mass of the Higgs and the mass of some would-be resonances, i.e., $m_h \equiv m_H \sim 125$ GeV, $m_\rho = 200, 750, 2000$ GeV respectively. The stability conditions put already some constraints on the couplings of the model which are $\lambda_\phi > 0$, $\lambda_H > 0$ and $\lambda_\phi \lambda_H > 6g_H^2$ (if $g_H < 0$).

It is most convenient to write out the quartic couplings in terms of the physical

masses of the scalars and the mixing angle in following way,

$$\lambda_H = \frac{m_\rho^2 \sin^2\theta + m_h^2 \cos^2\theta}{2v_H^2}\,,$$

$$\lambda_\phi = \frac{m_\rho^2 \cos^2\theta + m_h^2 \sin^2\theta}{v_\phi^2/3}\,,$$

$$g_H = \frac{m_\rho^2 - m_h^2}{4v_H v_\phi}\sin 2\theta\,.$$

Since m_h and v_H are known and in this work we will choose $m_\rho = 200, 750, 2000$ GeV, we then take the set $\{\theta, v_\phi, g_\chi, c_g, c_\gamma\}$ as free parameters.

3 Partial Decay Widths

We calculate the relevant partial decay widths when the interaction Lagrangian consists of two effective operators together with a Higgs portal. In this case, the pseudoscalar mixes with the SM Higgs. Therefore, the pseudoscalar decay channels additionally incorporate all the decay modes of the SM Higgs multiplied by a factor depending on the mixing angle. All possible pseudoscalar decay modes are $\rho \to \chi\chi$, $\gamma\gamma$, gg, W^+W^-, ZZ, $Z\gamma$, hh, $f\bar{f}$, where fermions in the SM are denoted by f. The decay width of the pseudoscalar when decays into a pair of DM is

$$\Gamma_\chi = \Gamma(\rho \to \bar{\chi}\chi) = \frac{g_\chi^2 m_\rho \cos^2\theta}{8\pi}(1 - \frac{4m_{\rm DM}^2}{m_\rho^2})^{1/2}\,, \tag{6}$$

where θ is the mixing angle defined in the previous section.

Let us now consider the decay of a pseudoscalar to $\gamma\gamma$ and gg. Due to the mixing with the SM Higgs, the pseudoscalar decay into two photons occurs not only through contact interaction but also can occur through loop processes induced predominantly via $W^\pm$ bosons and heavy fermions, in particular the top quark. Taking into account both effects, the resulting decay width reads

$$\Gamma_\gamma = \Gamma(\rho \to \gamma\gamma) = (\frac{\alpha_{\rm em}}{4\pi})^2 \frac{m_\rho^3}{16\pi v_H^2}|\mathcal{F}|^2\,, \tag{7}$$

where,

$$\mathcal{F} = \mathcal{F}_W(\beta_W)\sin\theta + \sum_f N_c Q_f^2 \mathcal{F}_f(\beta_f)\sin\theta + 64\,c_\gamma^2\cos\theta\,, \tag{8}$$

and $\beta_{f,W} = \frac{4m_{f,W}^2}{m_\rho^2}$. The loop functions $\mathcal{F}_W$ and $\mathcal{F}_f$ are defined as

$$\mathcal{F}_W(\beta) = 2 + 3\beta = 3\beta(2-\beta)f(\beta)\,,$$
$$\mathcal{F}_f(\beta) = -2\beta\Big(1 + (1-\beta)f(\beta)\Big)\,, \tag{9}$$

5

where,

$$f(\beta) = -\frac{1}{4}\left(\log(\frac{1 - \sqrt{1 + \beta}}{1 - \sqrt{1 - \beta}}) + i\pi\right)^2.\tag{10}$$

The pseudoscalar decay into two gluons is possible via an contact operator and through loop processes induced predominantly by heavy quarks. The final result for the decay width is

$$\Gamma_g = \Gamma(\rho \to gg) = \frac{\alpha_s^2 m_\rho^3}{72\pi^3 v_H^2}|\mathcal{F}|^2,\tag{11}$$

where,

$$\mathcal{F} = \sum_q \mathcal{F}_q(\beta_q)\sin\theta + 144\,c_g^2\cos\theta\tag{12}$$

and

$$\mathcal{F}_q(\beta) = \frac{3}{2}\beta(1 + (1 - \beta)f(\beta)).\tag{13}$$

For the rest of the decay modes we can apply the known formulas given for the relevant SM-Higgs decays which are now scaled by $\sin^2\theta$. The decay width for fermion emission is

$$\Gamma_f = \Gamma(\rho \to f\bar{f}) = \frac{N_c}{8\pi}\frac{m_f^2}{v_H^2}m_\rho\sin^2\theta(1 - 4x_f^2)^{3/2},\tag{14}$$

where $x_f = m_f/m_\rho$ and we set the color factor $N_c = 1$ for leptons and $N_c = 3$ for quarks.

The pseudoscalar can decay into $W^\pm$ gauge bosons with the following decay width

$$\Gamma_W = \Gamma(\rho \to W^+W^-) = \frac{1}{16\pi}\frac{m_\rho^3}{v_H^2}\sin^2\theta\sqrt{1 - 4x_W^2}(1 - 4x_W^2 + 12x_W^4),\tag{15}$$

where $x_W = m_W/m_\rho$. The pseudoscalar can decay into Z bosons with the decay rate

$$\Gamma_Z = \Gamma(\rho \to ZZ) = \frac{1}{32\pi}\frac{m_\rho^3}{v_H^2}\sin^2\theta\sqrt{1 - 4x_Z^2}(1 - 4x_Z^2 + 12x_Z^4),\tag{16}$$

where $x_Z = m_Z/m_\rho$. In our computations we apply the decay width $\Gamma_{Z\gamma} = \Gamma(\rho \to Z\gamma) \sim 10^{-3}\sin^2\theta$ GeV obtained from the exact formulas given in [9]. Finally, we present the partial decay width of the pseudoscalar into a pair of SM-Higgs bosons as

$$\Gamma_h = \Gamma(\rho \to hh) = \frac{\alpha^2}{8\pi m_\rho}\sqrt{1 - \frac{4m_h^2}{m_\rho^2}},\tag{17}$$

where $\alpha = (2\cos\theta - 6\cos\theta\sin^2\theta)g_H v_\phi + (4\sin\theta - 6\sin^3\theta)g_H v_H + \cos\theta\sin^2\theta\lambda_\phi v_\phi - 6(\cos^2\theta\sin\theta)\lambda_H v_H$.

4 The Constraints

In this section we discuss the LHC constraints, constraints from the oblique parameters and the observed relic density.

4.1 Higgs Physics Constraints

Two new decay channels for the SM Higgs boson will be possible in case $m_\rho < m_h/2$ and $m_{\rm DM} < m_h/2$. In the present work where $m_\rho = 200, 750, 2000$ GeV, only the decay $h \to \chi\chi$ can happen for small enough DM mass. Invisible Higgs decay investigations at the LHC put an upper limit on the invisible branching ratio, $\rm{Br}_{inv} \lesssim 0.24$ [10]. Applying this experimental bound we find,

$$|g_\chi \tan\theta| < \frac{5.04~({\rm MeV})^{1/2}}{(m_h^2 - 4m_\chi^2)^{1/4}}. \tag{18}$$

This will restrict our model parameter space in the regions with $m_{\rm DM} < m_h/2$.

On the other hand, an observable μ called signal strength which is measured by ATLAS and CMS has the Following definition,

$$\mu_i^f = \frac{\sigma_i \times {\rm Br}^f}{(\sigma_i \times {\rm Br}^f)_{\rm SM}}, \tag{19}$$

where σ_i is the Higgs production cross section via channel i and ${\rm Br}^f$ is the branching ratio of Higgs decaying into a final state f. Given various Higgs production and decay channels, the LHC best-fit result is $\mu = 1.09^{+0.11}_{-0.10}$ [11]. Due to the mixing between the SM Higgs and the singlet pseudoscalar in our model, σ_i is scaled by a factor $\cos^2\theta$ while ${\rm Br}^f$ remains the same as its SM value. Therefore, an upper limit of $\theta \lesssim 0.12$ on the mixing angle is found at 1σ level [12].

4.2 Oblique Parameters

For small mixing angle only the oblique parameter T is relevant. Following the discussion in [13], in the present model the parameter T is given by

$$T^{BSM} = -\left(\frac{3}{16\pi s_w^2}\right)\left\{ \cos^2\theta\left[\frac{1}{c_w^2}(\frac{m_h^2}{m_h^2 - m_Z^2})\ln\frac{m_h^2}{m_Z^2} - (\frac{m_h^2}{m_h^2 - m_W^2})\ln\frac{m_h^2}{m_W^2}\right] \right.$$
$$\left. + \sin^2\theta\left[\frac{1}{c_w^2}(\frac{m_\rho^2}{m_\rho^2 - m_Z^2})\ln\frac{m_\rho^2}{m_Z^2} - (\frac{m_\rho^2}{m_\rho^2 - m_W^2})\ln\frac{m_\rho^2}{m_W^2}\right]\right\}. \tag{20}$$

The quantity T is obtained in the SM by setting $\theta = 0$. The constraint from electroweak fit is given for $\Delta T = T^{BSM} - T^{SM}$ in [14] as $\Delta T = 0.01 \pm 0.12$. The oblique parameter puts insignificant constraint for small mixing angle of size $\theta \lesssim 0.1$.

4.3 Relic Density

In two experiments by Planck and WMAP, the relic density of DM is obtained. The combined result is $0.1172 < \Omega_{\mathrm{DM}} h^2 < 0.1226$ [15, 16]. An updated value for the relic density can be found in [17]. We will use this result to constrain the model parameter space. To this end, we need to solve numerically the Boltzmann equation,

$$\frac{dn_\chi}{dt} = -3H n_\chi - \langle \sigma_{\mathrm{ann}} v_{\mathrm{rel}} \rangle [n_\chi^2 - (n_\chi^{\mathrm{EQ}})^2] , \tag{21}$$

which provides us with the time evolution of DM number density and hence the present value of the density as a function of the thermal averaged annihilation cross section, $\langle \sigma_{\mathrm{ann}} v_{\mathrm{rel}} \rangle$.

To do the DM phenomenology we implement our model into the program MicrOMEGAs [18]. This package in turn employs the program CalcHEP [19] to compute the annihilation cross sections.

5 The Viable Parameter Space

In the present model any possible resonance is a pseudoscalar that plays the role of the mediator between the SM and the DM sectors. Having introduced two effective operators of dimension five, the DM annihilation channels are now $\chi\chi \to W^+ W^-, ZZ, hh, \bar{f}f, \gamma\gamma, gg$. The SM fermions are denoted by f. One question that we would like to address here is whether there can be viable regions in the DM sector which is consistent both with the constraints coming from the resonance of the mass $\sim 200, 750, 2000$ GeV with the decay width in the range $\Gamma^{\mathrm{tot}}/m_\rho \sim 0.03 - 0.06$, and constraints from observed relic density. We perform our computations for two sets of the effective couplings: $c_\gamma = 0.96, c_g = 0.027$ and $c_\gamma = 0.64, c_g = 0.0675$, with two values of the mixing angle, $\sin\theta = 0.01, 0.1$. In all cases we choose $v_\phi = 1000$ GeV.

Our numerical results for the two set of the effective couplings are shown in Fig. 1 for the DM mass being in the range 50 GeV up to 500 GeV, and for $\sin\theta = 0.01, 0.1$. It is evident from Fig. 1 that the role of the mixing angle is quite subtle in finding the DM mass range which gives both the relic density and the anticipated resonance decay width correctly. Let us look at the results for the large mixing angle, i.e., $\sin\theta = 0.1$. For the mediator mass, $m_\rho = 750$ GeV, there can be found DM candidates with mass ~ 65 GeV and $\sim 80 - 120$ GeV giving the observed relic density and the anticipated total decay width of the resonant. For the mediator mass, $m_\rho = 2000$ GeV, the viable region is $m_{\mathrm{DM}} = 65$ GeV and $m_{\mathrm{DM}} > 90$ GeV. For the smaller resonance mass, $m_\rho = 200$ GeV, the total decay width does not sit in the range $\Gamma^{\mathrm{tot}}/m_\rho \sim 0.03 - 0.06$ because the decay channels $\rho \to hh, t\bar{t}$ are no longer possible .

It can be seen readily that our results do not change much by going from one set of the couplings $\{c_\gamma, c_g\}$ to the other one.
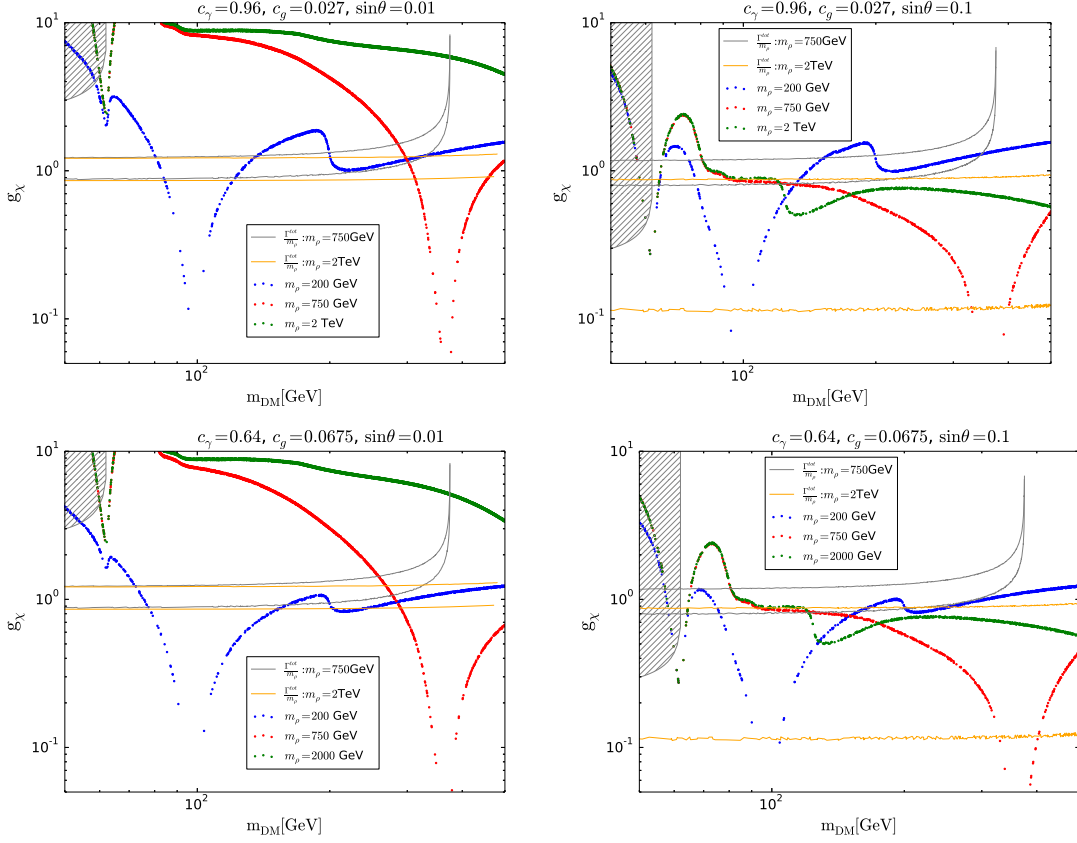
Figure 1: The DM mass against the dark coupling is shown with the mediator mass $m_\rho = 200, 750, 2000$ GeV respecting the WMAP/Planck relic density. The viable region is the intersection of the relic density line with the area of the total decay width $\Gamma^{\text{tot}}/m_\rho \sim 0.03 - 0.06$. The plots are drawn for two sets of effective couplings $c_\gamma = 0.96, c_g = 0.027$ and $c_\gamma = 0.64, c_g = 0.0675$ and two mixing angles $\sin\theta = 0.01, 0.1$. The total decay width bound for $m_\rho = 750$ GeV and $m_\rho = 2000$ GeV is the area between the gray lines and the orange lines, respectively. The shaded area is excluded by the invisible Higgs decay.

$\sqrt{s} = 13$ TeV	$\sqrt{s} = 8$ TeV
$\sigma(pp \to W^+W^-) < 300$ fb [20]	$\sigma(pp \to t\bar{t}) < 700$ fb [21]
$\sigma(pp \to ZZ) < 200$ fb [22]	$\sigma(pp \to gg) < 2.2$ pb [23]
$\sigma(pp \to Z\gamma) < 28$ fb [24]	
$\sigma(pp \to hh) < 120$ fb [25]	
$\sigma(pp \to \gamma\gamma) < 3$ fb ($m_\rho = 750$ GeV) [4]	
$\sigma(pp \to \gamma\gamma) < 0.3$ fb ($m_\rho = 2000$ GeV) [4]	

Table 1: Upper limits on the pp cross sections for various final states provided by LHC at $\sqrt{s} = 8, 13$ TeV.

6 Effective couplings consistent with the LHC bounds and the DM constraints

Assuming that a pseudoscalar resonance is responsible for the production of diboson and $t\bar{t}$ at the LHC, beyond the relevant background processes within the SM, we compute the various cross sections in terms of the introduced effective couplings, c_γ and c_g. To this end, we first implement our model into FeynRules [26] and then into MadGraph5 [27]. Four benchmark points, $c_\gamma = 0.96, c_g = 0.027$ and $c_\gamma = 0.64, c_g = 0.0675$ each with $m_{\text{DM}} = 100$ GeV, $m_\rho = 750$ GeV and $m_{\text{DM}} = 200$ GeV, $m_\rho = 2$ TeV are picked which already respect the observed relic density, $0.1172 < \Omega_{\text{DM}}h^2 < 0.1226$, and the anticipated pseudoscalar total decay width, $\Gamma^{\text{tot}}/m_\rho \sim 0.03 - 0.06$. We compare these four benchmark points against the observed upper limits on the cross sections, $pp \to W^+W^-, ZZ, \gamma\gamma, hh, gg, t\bar{t}$ at the LHC given in Table 1.

In Fig. 2 and Fig. 3 we present our main results for the above mentioned cross sections as contour plots and the corresponding upper limits against the effective couplings for $m_{\text{DM}} = 100$ GeV, $m_\rho = 750$ GeV and $m_{\text{DM}} = 200$ GeV, $m_\rho = 2$ TeV, respectively. In some plots the upper limits on the cross section reside beyond the range of the effective couplings or it is in a very small region and therefore are not visible. Strongest constraints come from the processes with $\gamma\gamma$ and gg in the final state for $m_\rho = 750$ GeV and for $m_\rho = 2$ TeV with $\gamma\gamma$, gg and hh in the final state.

Note that we have not included the process $pp \to Z\gamma$ in our plots. The reason is that $\Gamma(pp \to Z\gamma)$ is much smaller than $\Gamma(pp \to ZZ)$ as can be seen by comparing Eq. 16 and the relation $\Gamma(\rho \to Z\gamma) \sim 10^{-3} \sin^2\theta$ GeV. For instance when $m_\rho = 750$ GeV, $\Gamma_{ZZ}/\Gamma_{Z\gamma} \sim 280$. Given the upper limits for the two processes, $pp \to Z\gamma$ imposes much weaker constraints on the effective couplings.

7 Conclusion

The exciting report by ATLAS and CMS in 2015 [1, 2] on a 750 GeV excess in the diphoton events was nothing but a statistical fluctuation as announced by ATLAS 2016 report [4] and no significant excess was observed in 2016 data. Nevertheless the AT-
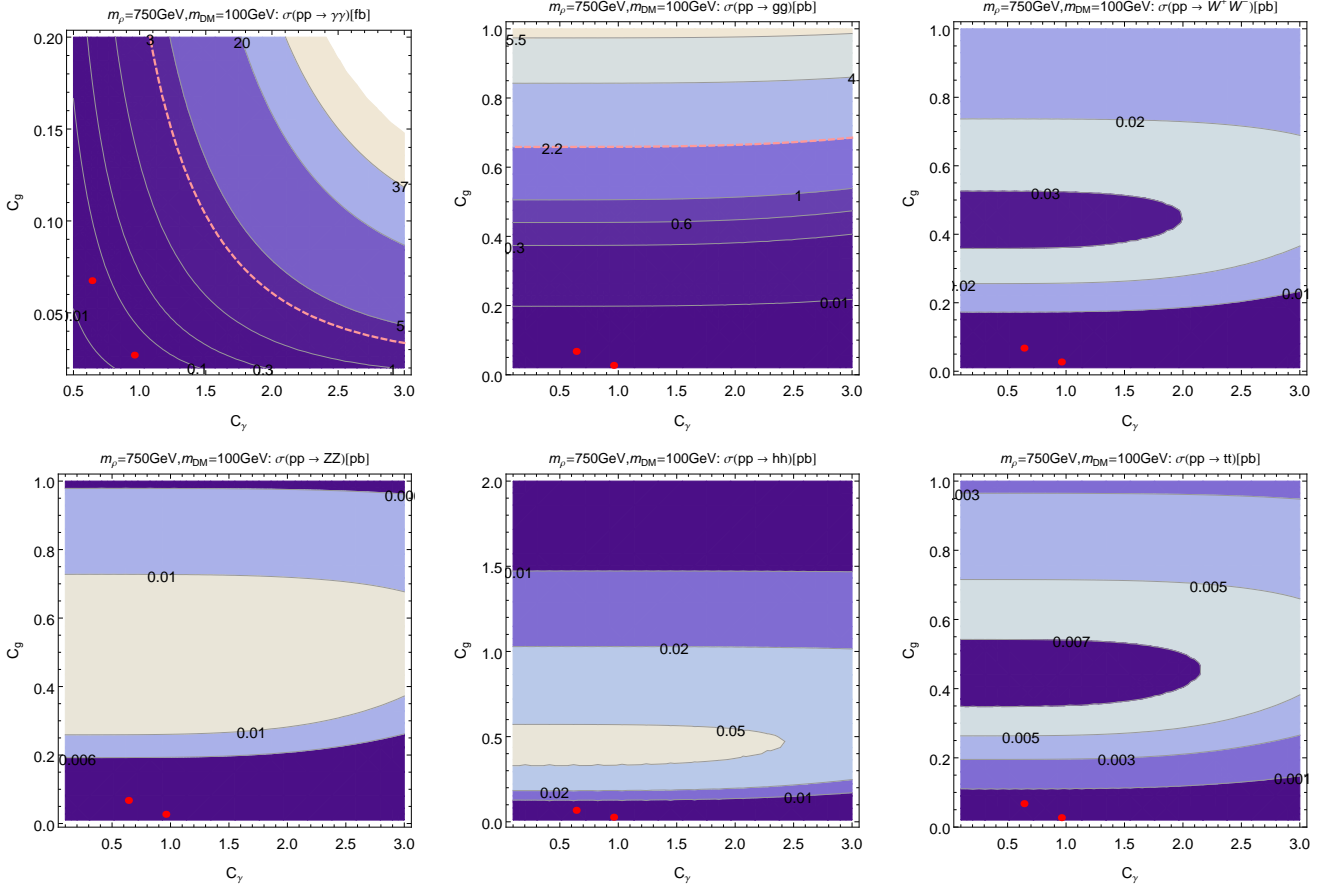
Figure 2: The contour plots illustrating the dependency of the various cross sections on the effective couplings with m_{DM}=100 GeV and m_{ρ}=750 GeV. The dashed line shows the LHC upper bound on the cross section. The red points are corresponding to two benchmarks $c_{\gamma} = 0.96, c_g = 0.027$ and $c_{\gamma} = 0.64, c_g = 0.0675$.
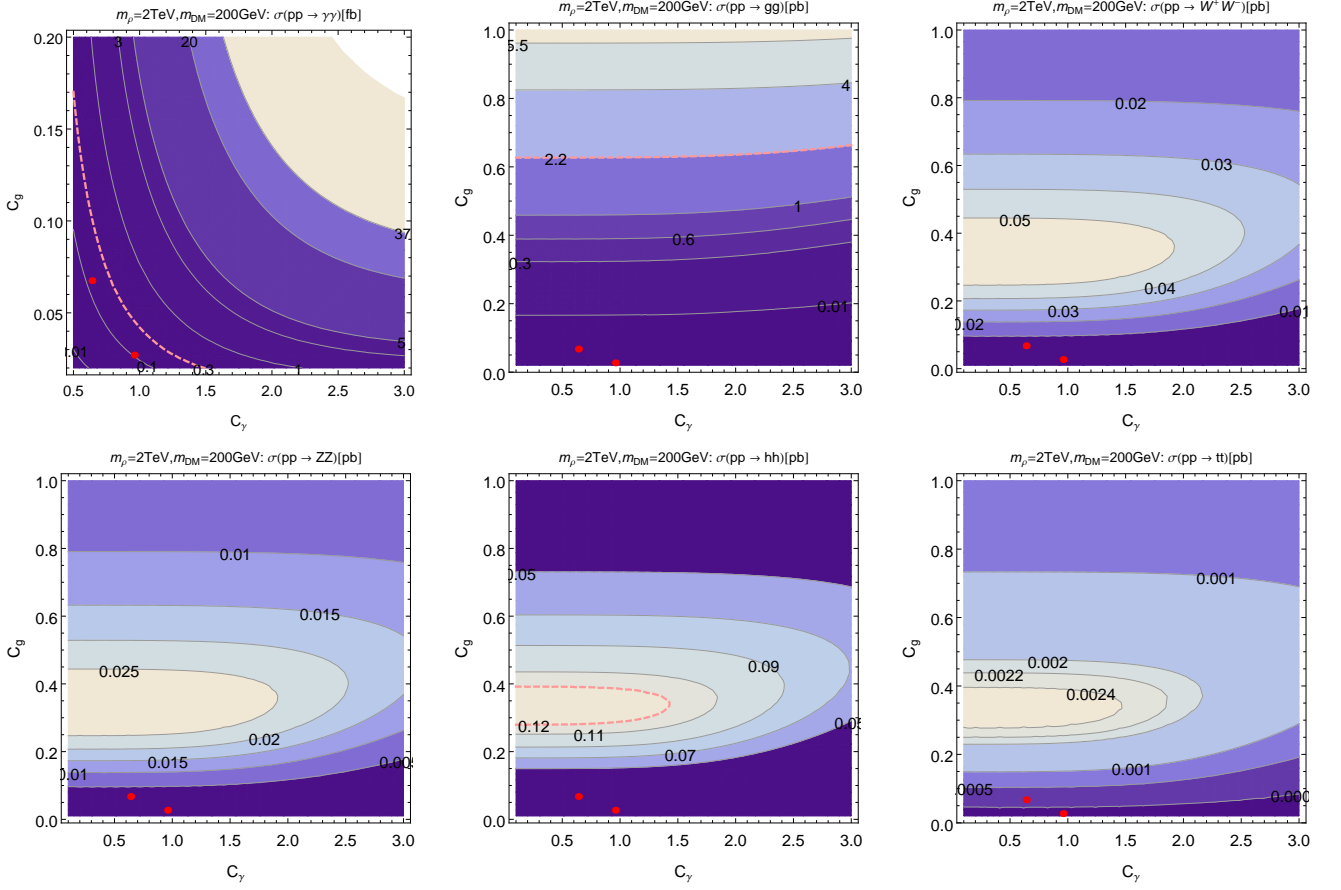
Figure 3: The contour plots illustrating the dependency of the various cross sections on the effective couplings with m_{DM}=200 GeV and m_ρ=2000 GeV. The dashed line shows the LHC upper bound on the cross section. The red points are corresponding to two benchmarks $c_\gamma = 0.96, c_g = 0.027$ and $c_\gamma = 0.64, c_g = 0.0675$.

LAS 2016 report provided an upper limit for the cross section of the diboson and $t\bar{t}$ in final state. In this paper we examined a fermionic dark matter scenario with a pseudoscalar mediator along with gluon and photon dimension five effective operators. The pseudoscalar plays the role of a spin-0 resonance which communicates with the standard model sector by the Higgs portal and couples also to the effective operators.

We have taken three masses for the spin-0 resonance being $m_\rho = 200, 750, 2000$ GeV and deal with two effective couplings c_g and c_γ. In Fig. 1 we have shown the viable DM mass for two sets of the effective couplings $\{c_g, c_\gamma\}$ and two mixing angles which fit with the observed relic density, invisible Higgs decay and gives the total decay width ratio $\Gamma^{\text{tot}}/m_\rho = 0.03 - 0.06$.

Then in contour plots Fig. 2 and Fig. 3 we have shown how the cross section for $pp \to W^+W^-, ZZ, \gamma\gamma, gg, t\bar{t}$ depends on the effective couplings for m_{DM}=100 GeV, m_ρ=750 GeV and m_{DM}=200 GeV, m_ρ=2000 GeV respectively. We have pinned down two benchmarks in each plot which fulfills all the constraints.

The characteristic of this fermionic dark matter model is that the DM-nucleon cross section is velocity suppressed because the mediator has been taken a pseudoscalar. The model therefore evades easily the bounds put by LUX [28] and XENON1T [29] or the future direct detection experiments.

References

[1] T. A. collaboration, "Search for resonances decaying to photon pairs in 3.2 fb^{-1} of pp collisions at $\sqrt{s} = 13$ TeV with the ATLAS detector,".

[2] **CMS** Collaboration, C. Collaboration, "Search for new physics in high mass diphoton events in proton-proton collisions at 13TeV,".

[3] **ATLAS** Collaboration, G. Aad *et al.*, "Observation of a new particle in the search for the Standard Model Higgs boson with the ATLAS detector at the LHC," *Phys. Lett.* **B716** (2012) 1–29, arXiv:1207.7214 [hep-ex].

[4] **ATLAS** Collaboration, T. A. collaboration, "Search for scalar diphoton resonances with 15.4 fb^{-1} of data collected at $\sqrt{s}$=13 TeV in 2015 and 2016 with the ATLAS detector,".

[5] M. A. Fedderke, J.-Y. Chen, E. W. Kolb, and L.-T. Wang, "The Fermionic Dark Matter Higgs Portal: an effective field theory approach," *JHEP* **08** (2014) 122, arXiv:1404.2283 [hep-ph].

[6] M. Cirelli, N. Fornengo, and A. Strumia, "Minimal dark matter," *Nucl. Phys.* **B753** (2006) 178–194, arXiv:hep-ph/0512090 [hep-ph].

[7] S. Baek, P. Ko, and W.-I. Park, "Search for the Higgs portal to a singlet fermionic dark matter at the LHC," *JHEP* **02** (2012) 047, arXiv:1112.1847 [hep-ph].

[8] K. Ghorbani, "Fermionic dark matter with pseudo-scalar Yukawa interaction," *JCAP* **1501** (2015) 015, `arXiv:1408.4929 [hep-ph]`.

[9] A. Djouadi, "The Anatomy of electro-weak symmetry breaking. I: The Higgs boson in the standard model," *Phys. Rept.* **457** (2008) 1–216, `arXiv:hep-ph/0503172 [hep-ph]`.

[10] **CMS Collaboration** Collaboration, "Searches for invisible Higgs boson decays with the CMS detector.," Tech. Rep. CMS-PAS-HIG-16-016, CERN, Geneva, 2016. `https://cds.cern.ch/record/2201136`.

[11] **ATLAS, CMS** Collaboration, G. Aad *et al.*, "Measurements of the Higgs boson production and decay rates and constraints on its couplings from a combined ATLAS and CMS analysis of the LHC pp collision data at $\sqrt{s} = 7$ and 8 TeV," `arXiv:1606.02266 [hep-ex]`.

[12] S. Ghosh, A. Kundu, and S. Ray, "Potential of a singlet scalar enhanced Standard Model," *Phys. Rev.* **D93** no. 11, (2016) 115034, `arXiv:1512.05786 [hep-ph]`.

[13] V. Barger, P. Langacker, M. McCaskey, M. J. Ramsey-Musolf, and G. Shaughnessy, "LHC Phenomenology of an Extended Standard Model with a Real Scalar Singlet," *Phys. Rev.* **D77** (2008) 035005, `arXiv:0706.4311 [hep-ph]`.

[14] **Particle Data Group** Collaboration, K. A. Olive *et al.*, "Review of Particle Physics," *Chin. Phys.* **C38** (2014) 090001.

[15] **Planck** Collaboration, P. A. R. Ade *et al.*, "Planck 2013 results. XVI. Cosmological parameters," *Astron. Astrophys.* **571** (2014) A16, `arXiv:1303.5076 [astro-ph.CO]`.

[16] **WMAP** Collaboration, G. Hinshaw *et al.*, "Nine-year wilkinson microwave anisotropy probe (wmap) observations: Cosmological parameter results," *Astrophys.J.Suppl.* **208** (2013) 19, `arXiv:1212.5226 [astro-ph]`.

[17] **Planck** Collaboration, P. A. R. Ade *et al.*, "Planck 2015 results. XIII. Cosmological parameters," *Astron. Astrophys.* **594** (2016) A13, `arXiv:1502.01589 [astro-ph.CO]`.

[18] G. Belanger, F. Boudjema, A. Pukhov, and A. Semenov, "micrOMEGAs3: A program for calculating dark matter observables," *Comput. Phys. Commun.* **185** (2014) 960–985, `arXiv:1305.0237 [hep-ph]`.

[19] A. Belyaev, N. D. Christensen, and A. Pukhov, "CalcHEP 3.4 for collider physics within and beyond the Standard Model," *Comput. Phys. Commun.* **184** (2013) 1729–1769, `arXiv:1207.6082 [hep-ph]`.

[20] "Search for WW/WZ resonance production in the $\ell\nu qq$ final state at $\sqrt{s} = 13$ TeV with the ATLAS detector at the LHC," Tech. Rep. ATLAS-CONF-2015-075, CERN, Geneva, Dec, 2015. `http://cds.cern.ch/record/2114847`.

[21] **ATLAS** Collaboration, G. Aad *et al.*, "A search for $t\bar{t}$ resonances using lepton-plus-jets events in proton-proton collisions at $\sqrt{s} = 8$ TeV with the ATLAS detector," *JHEP* **08** (2015) 148, `arXiv:1505.07018 [hep-ex]`.

[22] "Search for diboson resonances in the llqq final state in pp collisions at $\sqrt{s} = 13$ TeV with the ATLAS detector," Tech. Rep. ATLAS-CONF-2015-071, CERN, Geneva, Dec, 2015. `http://cds.cern.ch/record/2114843`.

[23] **CMS Collaboration** Collaboration, "Search for Resonances Decaying to Dijet Final States at $\sqrt{s} = 8$ TeV with Scouting Data," Tech. Rep. CMS-PAS-EXO-14-005, CERN, Geneva, 2015. `https://cds.cern.ch/record/2063491`.

[24] "Search for heavy resonances decaying to a Z boson and a photon in pp collisions at $\sqrt{s} = 13$ TeV with the ATLAS detector," Tech. Rep. ATLAS-CONF-2016-010, CERN, Geneva, Mar, 2016. `http://cds.cern.ch/record/2139795`.

[25] "Search for pair production of Higgs bosons in the $b\bar{b}b\bar{b}$ final state using proton-proton collisions at $\sqrt{s} = 13$ TeV with the ATLAS detector," Tech. Rep. ATLAS-CONF-2016-017, CERN, Geneva, Mar, 2016. `http://cds.cern.ch/record/2141006`.

[26] A. Alloul, N. D. Christensen, C. Degrande, C. Duhr, and B. Fuks, "FeynRules 2.0 - A complete toolbox for tree-level phenomenology," *Comput. Phys. Commun.* **185** (2014) 2250–2300, `arXiv:1310.1921 [hep-ph]`.

[27] J. Alwall, R. Frederix, S. Frixione, V. Hirschi, F. Maltoni, O. Mattelaer, H. S. Shao, T. Stelzer, P. Torrielli, and M. Zaro, "The automated computation of tree-level and next-to-leading order differential cross sections, and their matching to parton shower simulations," *JHEP* **07** (2014) 079, `arXiv:1405.0301 [hep-ph]`.

[28] **LUX** Collaboration, D. S. Akerib *et al.*, "Results from a search for dark matter in the complete LUX exposure," *Phys. Rev. Lett.* **118** no. 2, (2017) 021303, `arXiv:1608.07648 [astro-ph.CO]`.

[29] **XENON** Collaboration, E. Aprile *et al.*, "First Dark Matter Search Results from the XENON1T Experiment," `arXiv:1705.06655 [astro-ph.CO]`.